

# Charge Kondo Effect in Thermoelectric Properties of Lead Telluride doped with Thallium Impurities

T. A. Costi and V. Zlatić

**Abstract** We investigate the thermoelectric properties of PbTe doped with a small concentration  $x$  of Tl impurities acting as acceptors and described by Anderson impurities with negative on-site (effective) interaction. The resulting charge Kondo effect naturally accounts for a number of the low temperature anomalies in this system, including the unusual doping dependence of the carrier concentration, the Fermi level pinning and the self-compensation effect. The Kondo anomalies in the low temperature resistivity at temperatures  $T \leq 10$  K and the  $x$ -dependence of the residual resistivity are also in good agreement with experiment. Our model also captures the qualitative aspects of the thermopower at higher temperatures  $T > 300$  K for high dopings ( $x > 0.6\%$ ) where transport is expected to be largely dominated by carriers in the heavy hole band of PbTe.

## 1 Introduction

The ever growing demand for energy has increased interest in materials with high thermoelectric (TE) efficiency. A remarkable feature of TE devices is that they directly convert heat into electrical energy or use electricity to pump heat by circulating the electron fluid between a hot and a cold reservoir [1, 2]. The absence of mechanical parts makes TE devices very reliable but their low efficiency restricts applications to rather specialized fields. Today, they are mainly used in situations where reliability is the most important factor, e.g., for electricity generation in remote regions or for vibrationless cooling of sensitive devices.

---

T. A. Costi

Peter Grünberg Institut and Institute for Advanced Simulation, Research Centre Jülich, 52425 Jülich, Germany, e-mail: t.costi@fz-juelich.de

V. Zlatić

Institute of Physics, Zagreb POB 304, Croatia and J. Stefan Institute, SI-1000 Ljubljana, Slovenia  
e-mail: zlati@ifs.hr

The efficiency of TE materials is related to their figure-of-merit,  $ZT = P T / \kappa$ , where  $P$  is the power factor and  $\kappa$  is the thermal conductivity. Current applications are based on semiconducting materials that have a state-of-the-art  $ZT$  of around one [3, 4], which is not sufficient for wide-spread use. The production of cheap TE materials with a room temperature value of  $ZT \geq 2$  would be a major technological breakthrough.

The efforts to increase  $ZT$  follow two general strategies. The one tries to reduce  $\kappa$  and increase the efficiency by minimizing the thermal losses through the device. The other tries to increase  $P = S^2 \sigma$ , where  $S(T)$  is the Seebeck coefficient and  $\sigma(T)$  the electrical conductivity. Recent advances that achieved  $ZT \geq 2$  are mostly due to the reduction of  $\kappa$  by nanostructuring, i.e., by using multilayered materials (for review see [4]) and nanocomposites [5]. The enhancement of  $ZT$  via the power factor is less straightforward, because an increase of  $S(T)$  is usually accompanied by a reduction of  $\sigma$  and vice versa [6]. The reason is that  $\sigma(T)$  is mainly determined by the value of the density of states  $\mathcal{N}(\omega)$  and the transport relaxation time  $\tau(\omega)$  at the chemical potential  $\mu$ , while  $S(T)$  depends sensitively on the symmetry of  $\mathcal{N}(\omega)$  and  $\tau(\omega)$  around  $\mu$ . Thus, one way to a larger power factor is by increasing the asymmetry of  $\mathcal{N}(\omega)$  in the proximity of  $\mu$  by, say, confining the electron gas to low dimensions [7] or by introducing resonant states within the Fermi window by doping [8]. This strategy could work well for materials in which the charge carriers behave as non-interacting Fermions and the energy dependence of  $\tau(\omega)$  is negligibly small [9].

The other route to large  $P$  is via electron correlation which makes  $\tau(\omega)$  strongly energy dependent, as in heavy fermions [6, 10], e.g.,  $\text{YbAl}_3$ , transition metal oxides, e.g.  $\text{Na}_x\text{CoO}_2$  [11, 12], or in correlated semiconductors, such as  $\text{FeSi}$  [13, 14]. However, these materials have large  $\kappa$  such that  $ZT$  is too small for applications, except, perhaps, at very low temperatures. At high temperatures, the correlation effects are usually less pronounced and the appropriate materials are not easy to find. Considering the complexity of the problem, it is clear that the search for better thermoelectrics could benefit considerably from an understanding of basic microscopic mechanisms that govern the thermoelectric response of a given material.

One of the most interesting thermoelectric materials is  $\text{Pb}_{1-x}\text{Tl}_x\text{Te}$ , where  $x$  is the concentration of Tl impurities [15, 16, 17]. The parent compound  $\text{PbTe}$  is a narrow gap semiconductor with a gap of 190 meV and is itself a good thermoelectric material with a thermopower of around  $300 \mu\text{V/K}$  at 800 K. Upon doping with Tl impurities, which act as acceptors [15, 16], a large thermopower persists at high temperature, while a number of anomalies appear in the low temperature properties. Remarkable, these depend sensitively on the Tl concentration with a qualitatively different behavior below and above a critical concentration  $x_c \simeq 0.3$  at% Tl. For example,  $\text{Pb}_{1-x}\text{Tl}_x\text{Te}$  becomes superconducting for  $x > x_c$  with a transition temperature  $T_c(x)$  increasing linearly with  $x$  and reaching 1.5 K at  $x = 1.5$  at% Tl [18, 19]. This is surprisingly high given the low carrier density of  $10^{20}$  holes/cm<sup>3</sup>. Measurements of the Hall number  $p_H = 1/R_H e$  [19] indicate that the number of holes grows linearly with  $x$  for  $x \leq x_c$ , whereas for  $x > x_c$  the number of holes remains almost constant: the system exhibits “self-compensation” and the chemical potential is pinned to a value  $\mu \simeq \mu^* = 220 \text{ meV}$  [19, 20, 21]. Transport measure-

ments show anomalous behavior at low temperatures: while for  $x < x_c$ , the residual resistance  $\rho_0$  is very small and almost constant [22], for  $x > x_c$ ,  $\rho_0$  increases approximately linearly with  $x$ . For  $x < x_c$ , the resistivity,  $\rho(T)$  exhibits a positive slope at low temperature [23], while for  $x > x_c$ , the slope is negative and a Kondo like impurity contribution  $\rho_{\text{imp}}(T)$  is observed for  $T \leq 10$  K. The origin of this anomaly is not due to magnetic impurities, since the susceptibility is diamagnetic [23]. Finally, at low Tl concentrations,  $S(T)$  shows a sign-change before growing to large positive values at room temperatures [22].

Several models have been proposed to explain the anomalous properties of  $\text{Pb}_{1-x}\text{Tl}_x\text{Te}$ . The simplest assumes that doping with Tl gives rise to non-interacting resonant levels close to the top of the p-valence band of PbTe [15]. Density functional theory (DFT) calculations confirm the presence of such states with Tl  $s$ -character [24]. In the static mixed valence model [25, 16], Tl impurities, known to be valence skippers in compounds, are assumed to dissociate into energetically close  $\text{Tl}^{1+}$  ( $6s^2p^1$ ) and  $\text{Tl}^{3+}$  ( $6s^0p^3$ ) ions, while the  $\text{Tl}^{2+}$  ( $6s^1p^2$ ) configuration lies higher in energy (consistent with DFT calculations [26]). With a strong electron-phonon interaction such a model results in negative on-site  $U$ . This model provides a natural explanation for the observed self-compensation and the diamagnetic behavior of  $\text{Pb}_{1-x}\text{Tl}_x\text{Te}$  [25]. In addition, it provides a mechanism for the onset of superconductivity. Dynamic fluctuations between the  $\text{Tl}^{1+}$  and  $\text{Tl}^{3+}$  valence states results in the negative  $U$  Anderson model [27] which supports a charge Kondo effect [28, 29] and has been proposed to explain the anomalous properties of  $\text{Pb}_{1-x}\text{Tl}_x\text{Te}$  [23, 19, 22, 30, 31, 32, 33], including the superconductivity for  $x > x_c$  [31, 32]. A coupling of the Tl ions to the lattice has also been considered [34, 35]. Recent ARPES data on a 0.5% sample [36] are also consistent with a negative  $U$  Anderson model.

As regards the thermoelectric properties of interest for applications, increasing the Tl concentration beyond 1 at% gives rise to a room-temperature  $ZT$  which is surprisingly large for a bulk material [17]. The data show that the thermopower  $S(T)$  increases almost linearly at low temperatures [22] and saturates above 400 K at rather high values [17]. The fact that the enhancement of  $ZT$  occurs at high temperatures and that it is mainly due to an increased power factor makes this material particularly interesting not just from the practical but also from the theoretical point of view.

In this paper, we use the numerical renormalization group approach (NRG) [37] to calculate the anomalous frequency and temperature dependent transport time,  $\tau(\omega, T)$ , of electrons scattering from Tl impurities described as negative- $U$  Anderson impurities. We show that this model explains the unusual concentration and temperature dependent properties of  $\text{Pb}_{1-x}\text{Tl}_x\text{Te}$ . We take full account of charge neutrality and include the realistic band structure of PbTe [9]. We find that both correlation and band effects are important in accounting for the experimental data. We shall also show, that our single-band Anderson impurity model qualitatively reproduces the measured behaviour of the thermopower over a wide temperature range in the regime where transport is mainly due to carriers in a single heavy hole like sub-band of the PbTe valence band. At lower dopings, the population of two valence

sub-bands of PbTe requires a further generalization of the model in order to describe the thermopower also in this regime (see discussion in Sec. 9). This, however, is beyond the scope of the present paper.

## 2 Negative- $U$ Anderson Model for Tl impurities in PbTe

We consider  $n$  Tl impurities in a PbTe crystal with  $N$  Pb sites described by the Hamiltonian  $H = H_{\text{band}} + H_{\text{imp}} + H_{\text{hyb}}$ , where

$$H_{\text{band}} = \sum_{\mathbf{k}\sigma} (\epsilon_{\mathbf{k}} - \mu) c_{\mathbf{k}\sigma}^\dagger c_{\mathbf{k}\sigma} , \quad (1)$$

$$H_{\text{imp}} = (\epsilon_0 - \mu) \sum_{i=1}^n \hat{n}_{i\sigma} + U \sum_{i=1}^n n_{i\uparrow} n_{i\downarrow} , \quad (2)$$

$$H_{\text{hyb}} = \sum_{i=1}^n \sum_{k\sigma} V_{\mathbf{k}} (c_{\mathbf{k}\sigma}^\dagger s_{i\sigma} + h.c.) . \quad (3)$$

$c_{\mathbf{k}\sigma}^\dagger$  creates an electron in the valence p-band at energy  $\epsilon_{\mathbf{k}}$ ,  $\hat{n}_{i\sigma} = s_{i\sigma}^\dagger s_{i\sigma}$  is the number operator for a Tl  $s$ -electron at site  $i$  with spin  $\sigma$  and energy  $\epsilon_0$ ,  $U$  is the (negative) on-site interaction, and  $V_{\mathbf{k}}$  is the matrix element for the  $s$ - $p$  interaction. Its strength is characterized by the hybridization function  $\Delta(\omega) = \pi \sum_{\mathbf{k}} |V_{\mathbf{k}}| \delta(\omega - \epsilon_{\mathbf{k}})$ . We neglect the  $\mathbf{k}$ -dependence of  $V_{\mathbf{k}}$  setting  $V_{\mathbf{k}} = V_0$  but keep the full energy dependence of  $\Delta(\omega)$  by using the p-band density of states  $\mathcal{N}(\omega) = \sum_{\mathbf{k}} \delta(\omega - \epsilon_{\mathbf{k}})$  calculated from DFT and including relativistic effects [9]. The chemical potential  $\mu$  determines  $n_e = \frac{1}{N} \sum_{\mathbf{k}\sigma} \langle c_{\mathbf{k}\sigma}^\dagger c_{\mathbf{k}\sigma} \rangle$  and  $n_s = \frac{1}{n} \sum_{i=1}^n \sum_{\sigma} \langle n_{i\sigma} \rangle$ , the average number of  $p$  and  $s$  electrons per site. We denote by  $x = n/N$  the concentration of Tl impurities. Since Tl acts as an acceptor, the ground state corresponds to the  $\text{Tl}^{1+}$  ( $n_s = 2$ ) configuration and the  $\text{Tl}^{3+}$  ( $n_s = 0$ ) configuration is split-off from the ground state by the energy  $\delta = E(\text{Tl}^{3+}) - E(\text{Tl}^{1+}) > 0$ . A concentration  $x$  of Tl impurities accommodates  $x(n_s - 1)$  electrons (per Tl site), where the number of accepted electrons in the  $6s$  level of Tl is measured relative to the neutral  $\text{Tl}^{2+}$  ( $s^1$ ) configuration having  $n_s = 1$ . These electrons are removed from the valence band leaving behind  $n_0 = 1 - n_e$  holes. Thus, the charge neutrality condition reads [32]

$$n_0 = x(n_s - 1) , \quad (4)$$

which for a given  $x$  and temperature  $T$  has to be satisfied by adjusting the hole chemical potential  $\mu$ . Here, we neglect inter-impurity interactions and solve  $H$  for a finite number of independent negative- $U$  centres by using the NRG [37]. For each  $x$  and each  $T$  we need to satisfy (4) by self-consistently determining the chemical potential. In practice we found it more efficient to solve the negative- $U$  Anderson model on a dense grid of 256 chemical potentials about  $\mu = \mu^*$  and to subsequently convert these by interpolation to a fixed particle number (i.e. obeying Eq. (4) for each  $T$  at given  $x$ ).

### 3 Transport coefficients

The transport coefficients for scattering from a dilute concentration  $x$  of Tl impurities are obtained from the Kubo formula [38]. The electrical resistivity and the thermopower are defined by the usual expressions,

$$\rho_{\text{imp}}(T) = \frac{1}{e^2 L_{11}}, \quad (5)$$

$$S(T) = -\frac{1}{|e|T} \frac{L_{12}}{L_{11}}, \quad (6)$$

where  $L_{11}$  and  $L_{12}$  are given by the static limits of the current-current and current-heat current correlation functions, respectively. In the absence of non-resonant scattering the vertex corrections vanish and the transport integrals can be written as [38, 39],

$$L_{ij} = \sigma_0 \int_{-\infty}^{\infty} d\omega \left( -\frac{df(\omega)}{d\omega} \right) \mathcal{N}(\omega) \tau(\omega, T) \omega^{i+j-2}, \quad (7)$$

where  $\sigma_0$  is a material-specific constant,  $f(\omega) = 1/[1 + \exp(\omega/k_B T)]$  is the Fermi function,  $\tau(\omega, T)$  is the conduction-electron transport time[39]

$$\frac{1}{\tau(\omega, T)} = 2\pi c_{\text{imp}} V_0^2 A(\omega, T), \quad (8)$$

and  $A(\omega, T) = \mp \frac{1}{\pi} \text{Im } G(\omega \pm i0^+)$  is the spectral function of  $s$ -holes. The number of Tl impurities  $c_{\text{imp}}$  per  $\text{cm}^3$  is related to  $x$  in % by  $c_{\text{imp}} = 1.48 \times 10^{20} x$  (using the lattice constant  $a_0 = 6.46 \times 10^{-8} \text{cm}$  of the PbTe rocksalt structure). Eqs.(7) and (8) show that  $\rho_{\text{imp}}(T)$  depends strongly on the value of  $A(\omega, T)$  around  $\omega \simeq \mu$  and that the sign and the magnitude of  $S(T)$  follow from the shape of  $\mathcal{N}(\omega)A(\omega, T)$  within the Fermi window  $|\omega| \leq 2k_B T$ . Since PbTe has an unusual non-parabolic band structure close to the top the valence band [9], and since this region is accessible with Tl dopings  $x \leq 1\%$ , one sees that the thermopower in particular will be sensitive to details of both  $\mathcal{N}(\omega)$  and  $A(\omega, T)$ .

### 4 Choice of Model Parameters

Low temperature Hall effect and tunneling experiments for samples with  $x > x_c$  provide an estimate for  $\mu^* \approx 220 \text{meV}$  that we use. Other parameters such as  $\Delta_0 = \Delta(\mu^*)$ , required to fix the hybridization function  $\Delta(\omega)$ , and  $U$  are unknown, or they depend strongly on the interpretation of experiments (see discussion below). However, the measured Kondo-like resistivity for  $x \geq x_c$  at low temperatures requires that  $|U| \gg \Delta_0$ . We take  $U/\Delta_0 = -8$ . As argued in [33], it is possible to estimate  $U$  and  $\Delta_0$  by interpreting the point contact measurements [20] within our model and by assuming that the Kondo scale  $T_K$  in the resistivity anomaly

at large dopings is comparable to the  $T_c \sim 1.5\text{K}$ , resulting in  $U = -30\text{meV}$  and  $\Delta = 2.7\text{meV}$ . While, the precise values of these parameters are required to consistently explain all measurements, in this paper we shall choose different values to those in [33] in order to substantiate the claim made there, that the qualitative aspects of those results remain the same for  $10\text{meV} \leq |U| \leq 220\text{meV}$  (and  $U/\Delta_0 = -8$ ). Hence, we shall choose  $\Delta_0 = 13.75\text{meV}$  and  $U = -110\text{meV}$  resulting in  $T_K \approx 14\text{K}$ , where the Kondo scale  $T_K$  is defined via the resistivity  $\rho_{\text{imp}}(T_K) = \rho_{\text{imp}}(T=0)/2$  for  $x \gg x_c$ . This is the same order of magnitude as the perturbative scale  $T'_K = \Delta_0(U/2\Delta_0)^{1/2} \exp(-\pi U/8\Delta_0) = 0.0864\Delta_0$  for the negative- $U$  Anderson model [29, 40].

## 5 Qualitative considerations

Before presenting our results, it is instructive to consider the atomic limit  $V_0 = 0$ . For  $x = 0$  the chemical potential lies in the gap between the valence and conduction bands. For finite but very small  $x$  each Tl impurity accepts one electron, i.e.  $n_s \approx 2$  and  $n_0 \approx x$  grows linearly with  $x$ . At the same time, the chemical potential shifts downwards into the valence band  $\mu < E_v$ , where  $E_v$  denotes the top of the valence band. This implies that the splitting  $\delta(\mu) = -(2(\epsilon_0 - \mu) + U)$  between donor and acceptor configurations *decreases*. Eventually, at a critical concentration  $x = x_c$ , the chemical potential reaches  $\mu = \mu^* = \epsilon_0 + U/2$  where  $\delta(\mu) = 2(\mu - \mu^*)$  vanishes and the system is in a mixed valence state where the  $\text{TI}^{1+}$  and  $\text{TI}^{3+}$  configurations are degenerate. In this situation  $n_s = 1$ , and any further doping with Tl cannot increase the hole carrier density beyond the value  $n_0(\mu^*)$ , i.e. one has self-compensation with a pinning of the chemical potential to  $\mu^*$  [32]. Experiments show that the properties of  $\text{Pb}_{1-x}\text{Tl}_x\text{Te}$  change dramatically for  $x > x_c \approx 0.3\%$  but a static mixed valence state implied by the above atomic limit cannot capture many of these, for example, the anomalous upturn of the resistivity at  $T < 10\text{K}$ .

For finite  $V_0$ , quantum fluctuations between the degenerate states  $\text{TI}^{1+}$  and  $\text{TI}^{3+}$  at  $\mu = \mu^*$  become important and lead to a charge Kondo effect [28]. This significantly affects all static and dynamic properties [29] and needs to be taken into account in describing the experiments. This charge Kondo effect is important also for  $\mu > \mu^*$ , since a finite charge splitting  $\delta(\mu) > 0$  in the negative- $U$  Anderson model is similar to a Zeeman splitting in the conventional spin Kondo effect [41]. The latter is known to drastically influence all properties. Thus, for the whole range of concentrations  $x$ , one expects dynamic fluctuations to play an important role in the properties of  $\text{Pb}_{1-x}\text{Tl}_x\text{Te}$ .

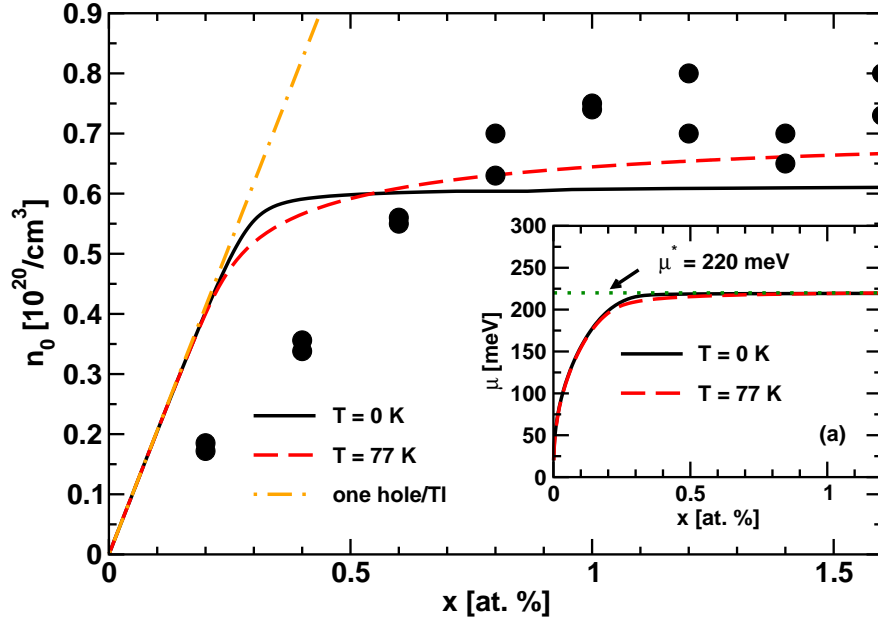


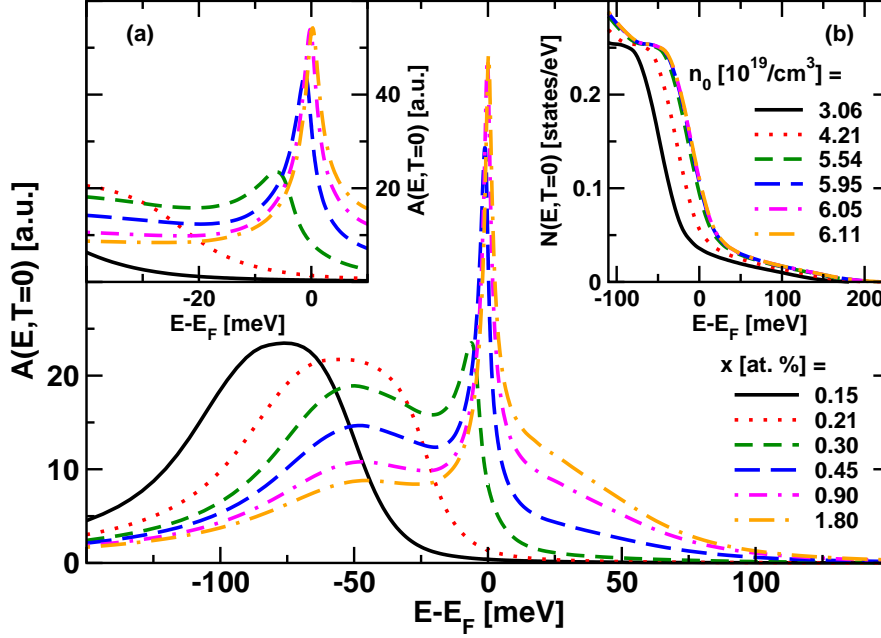
**Fig. 1** Hole carrier density  $n_0$  versus Tl doping  $x$  in atomic % (at. %) for  $T = 0$  K and  $T = 77$  K. The dot-dashed line is the hypothetical  $n_0$  for one hole per Tl. Filled circles are experimental data from Hall number measurements at  $T = 77$  K [20]. Inset (a): hole chemical potential  $\mu$  versus  $x$  at  $T = 0$  K and  $T = 77$  K (dotted line indicates value of the pinned chemical potential  $\mu^* = 220$  meV). The value of the charge splitting  $\delta(\mu) = 2(\mu - \mu^*)$  can also be read off from this plot.

## 6 Carrier Concentration

Figure 1 shows the hole carrier density  $n_0(x)$  versus Tl concentration  $x$  (in %) at  $T = 0$  and at  $T = 77$  K. For  $x < x_c \approx 0.3$ ,  $n_0$  is linear in  $x$ , i.e. each Tl contributes one hole, as in the case of vacancies on Pb sites (dot-dashed curve in Fig. 1). For  $x > x_c \approx 0.3$ ,  $n_0(x)$  saturates rapidly with increasing  $x$  for  $T = 0$  and more slowly at finite temperature. The hole chemical potential  $\mu$ , shown in Fig. 1a, grows non-linearly with  $x$  at  $x < x_c$  and rapidly approaches the value  $\mu^* = 200$  meV for  $x > x_c$ , both at  $T = 0$  and at  $T = 77$  K. Both of these results are in good qualitative agreement with experimental data [20] (see [33] for comparisons to more data [19]). Since we use the realistic band structure, we are also able to obtain quantitative agreement for the saturation density  $n_0 \approx 0.7 \times 10^{20}/\text{cm}^3$ . The self-compensation effect at  $x \gg x_c$  is a “smoking gun” signature for the charge Kondo state: on entering this state, the Tl ions fluctuate between  $\text{Tl}^{1+}$  and  $\text{Tl}^{3+}$  so the average valence  $\text{Tl}^{2+}$  is neither a donor nor an acceptor and the carrier density ceases to increase for  $x > x_c$ . Counter-doping with donor ions, removes holes, increases  $\mu$  and the charge splitting and consequently destroys the charge Kondo state. Indeed, counter-doping with In, a

donor ion, has been shown to destroy the charge Kondo anomalies in the resistivity and the onset of superconductivity [30]

## 7 TI $s$ -Electron Spectral Function



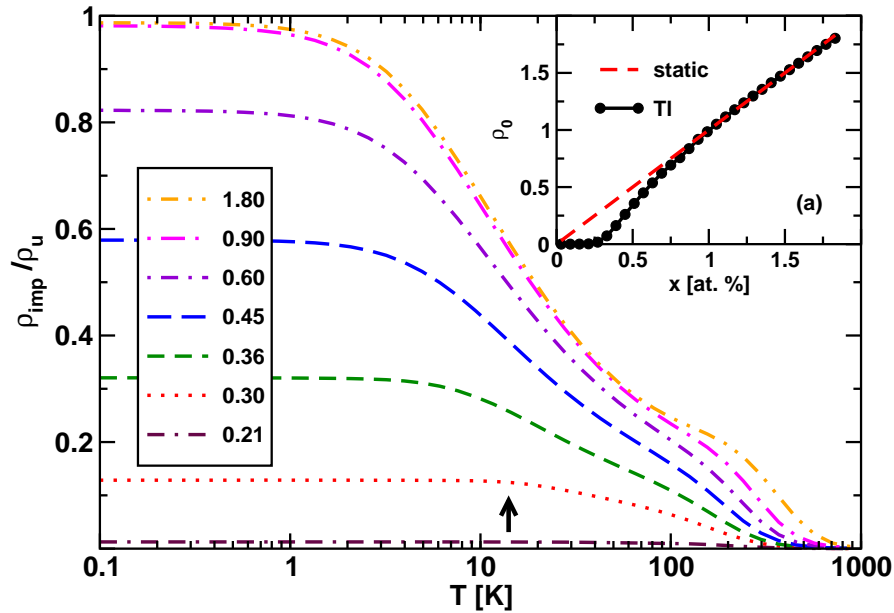
**Fig. 2** Main panel:  $T = 0$  spectral function  $A(E, T = 0)$  versus energy  $E - E_F$  for a range of TI dopings  $x$ . Here,  $E_F = E_F(x)$  is the self-consistently calculated Fermi level for each  $x$ . Inset (a): region near  $E = E_F$  showing the charge Kondo resonance. Inset (b): valence band local density of states  $\mathcal{N}(E)$  versus  $E - E_F$  for  $x$  as in the main panel. The conduction band (not shown) lies 190 meV above the top of the valence band and is not important for the present study. The hole carrier densities  $n_0$  for each  $x$ , obtained from Fig. 1, are given in the legend.

Figure 2 shows the evolution with TI doping of the single-particle spectral function  $A(E, T = 0)$  at zero temperature. For small doping, the hole chemical potential  $\mu$  lies above  $\mu^*$ , within the shallow part of the valence band density of states (see inset Fig. 2b), and consequently the splitting  $\delta(\mu) = 2(\mu - \mu^*)$  is large. A large charge splitting in the negative- $U$  Anderson model acts like a large Zeeman splitting in the corresponding positive- $U$  model. Consequently for  $x \ll x_c$ , the spectral function is strongly polarized, with most weight lying in a Hubbard satellite peak far below the Fermi level  $E_F$  with no other peaks in the spectral function. With increasing  $x$ , the charge splitting  $\delta(\mu)$  decreases, the spectral function becomes less



polarized, and for  $x \geq x_c$ , in addition to the Hubbard peak discussed above, a charge Kondo resonance develops close to  $E_F$ . The latter is a result of dynamic valence fluctuations between the almost degenerate  $\text{Tl}^{1+}$  and  $\text{Tl}^{3+}$  configurations. Point contact measurements for PbTe samples doped with  $x > x_c$  show the existence of two quasi-localized states [20], a narrow one of width 6 meV close to the Fermi level and a broader one of width 12 meV further below the Fermi level, in broad agreement with our theoretical calculations [33]. Indeed, in [33], this interpretation of the experiments was used to estimate  $U$  from the separation of the lower Hubbard band from the Kondo resonance.

## 8 Resistivity Anomaly



**Fig. 3** Normalized impurity contribution to the resistivity  $\rho_{\text{imp}}(T)/\rho_u$  versus temperature  $T$  and a range of Tl concentrations  $x$  (in %, see legend). Note that for  $T > 10$  K, the total resistivity will be dominated by the phonon contribution, not shown in this figure.  $\rho_u = 2c_{\text{imp}}/(e^2\pi\hbar N_F^2\sigma_0)$  is the residual resistivity for unitary scatterers with  $N_F = N(\mu^*)$  the density of valence band states at  $\mu = \mu^*$  and  $\sigma_0$  a material dependent constant. The vertical arrow indicates the Kondo temperature  $T_K = 14$  K at the charge Kondo degeneracy point. Inset (a): residual resistivity  $\rho_0 = x\rho_{\text{imp}}(T=0)/\rho_u$  versus  $x$  (filled circles). Dashed-line: residual resistivity for static impurities in place of Tl.

The temperature and doping dependence of the impurity resistivity,  $\rho_{\text{imp}}$ , is shown in Fig. 3. For  $x < x_c$ , Tl impurities act as acceptors with a well-defined va-

lence state ( $\text{TI}^{1+}$ ). They therefore act as weak potential scatterers and consequently the resistivity is much below the unitary value, as seen in Fig. 3. For  $x > x_c$ , dynamic fluctuations between the nearly degenerate  $\text{TI}^{1+}$  and  $\text{TI}^{3+}$  states leads to the charge Kondo effect and  $\rho_{\text{imp}}$  approaches the resistivity for unitary scatterers at  $T = 0$ . For  $x > x_c$ ,  $\rho_{\text{imp}}$  is well described by the *spin* Kondo resistivity [33] with a logarithmic form around  $T \approx T_K^{\text{eff}}$ , where  $T_K^{\text{eff}}$  is an effective Kondo scale, and  $T^2$  Fermi liquid corrections at low  $T \ll T_K^{\text{eff}}$ , in qualitative agreement with experiment [23]. The effective Kondo scale  $T_K^{\text{eff}}$  is a function of the charge splitting  $\delta(\mu)$  and  $T_K$ , and approaches the true Kondo scale  $T_K$  only asymptotically for  $x \gg x_c$  (see legend to Fig. 3). Finally, Fig. 3a shows that the impurity residual resistivity is significant only when the charge Kondo effect is operative, i.e. for  $x > x_c$ , in qualitative agreement with experiment [23, 22].

## 9 Thermopower

In Figure 4 we show the temperature dependence of the thermopower  $S(T)$  for several TI concentrations in the highly doped regime. At low temperature  $T \ll T_K$ , the thermopower can be obtained from a Sommerfeld expansion of Eq. (6),

$$S(T) = -\frac{\pi^2 k_B}{3|e|} k_B T \left( \frac{\mathcal{N}'(E_F)}{\mathcal{N}(E_F)} - \frac{A'(E_F)}{A(E_F)} \right), \quad (9)$$

where the first term is the band contribution to the thermopower and the second term involving the TI *s*-electron spectral function is that due to the charge Kondo effect of the TI impurities. Since TI ions act as acceptors, the TI *s*-electron spectral function,  $A(E)$ , has most of its weight below  $E_F$  and its slope at  $E_F$ , like that of  $\mathcal{N}(E)$ , is negative (see Fig. 2 and Fig. 2b). Consequently, at low temperature, the charge Kondo and band contributions to the thermopower are both *p*-type and compete with each other. This implies that thermopower can undergo a sign change at low temperature, depending on details, such as the TI doping level. Recent measurements show the occurrence of such sign changes at low TI dopings [22] consistent with a charge Kondo effect. However, our effective single band Anderson model for TI ions in PbTe is not accurate enough to describe the details of these sign changes, for the following reason. The valence *p*-band of PbTe actually consists of two sub-bands, light and heavy hole bands due to different hole pockets in the Brillouin zone [42]. These bands with densities of states  $\mathcal{N}_1(E)$  and  $\mathcal{N}_2(E)$  become successively occupied with increasing TI doping, and for  $x \approx x_c$  there is significant population of both. For simplicity, in Sec. 2 the effect of both bands was approximated only in the density of states  $\mathcal{N}(E) = \mathcal{N}_1(E) + \mathcal{N}_2(E)$ . For transport properties, such as thermopower, which depend sensitively on the relative populations and mobilities of such sub-bands, an effective one band model is, in general, not adequate. We expect, however, that it is approximately correct in the high doping limit when transport is mainly due carriers in the heavy hole band. In this limit, and at temperatures  $T \gg T_K$ ,

when the charge Kondo effect is suppressed, our results for  $S$  should reproduce those from just the band contribution ( $\mathcal{N}(E)$ ) within a constant relaxation time approximation  $\tau(E, T) = \tau_0$  [9]. Fig. 4 shows that this is indeed the case for  $x > 0.9\%$  and  $T \geq 175\text{K}$ . The large thermopower in the range  $300 - 800\text{K}$  increases with decreasing carrier density, reflecting the enhancement of  $\mathcal{N}'(E_F)/\mathcal{N}(E_F)$  with increasing  $E_F$  (i.e. *decreasing* hole chemical potential  $\mu$ ). In Fig. 4b we show the electronic figure of merit  $z_0T = PT/\kappa_e$ , where  $\kappa_e$  is the electronic thermal conductivity. The quantity  $z_0T$  is an upper bound to the true figure of merit  $ZT$ . We find  $z_0T = 2$  and  $z_0T = 4$  at  $T = 800\text{K}$  for  $x \approx 1\%$  and  $x \approx 2\%$ , respectively, approximately twice larger than the reported measured values of  $ZT$  at the same temperature and doping levels[17]. This is reasonable, given our neglect of the lattice thermal conductivity.

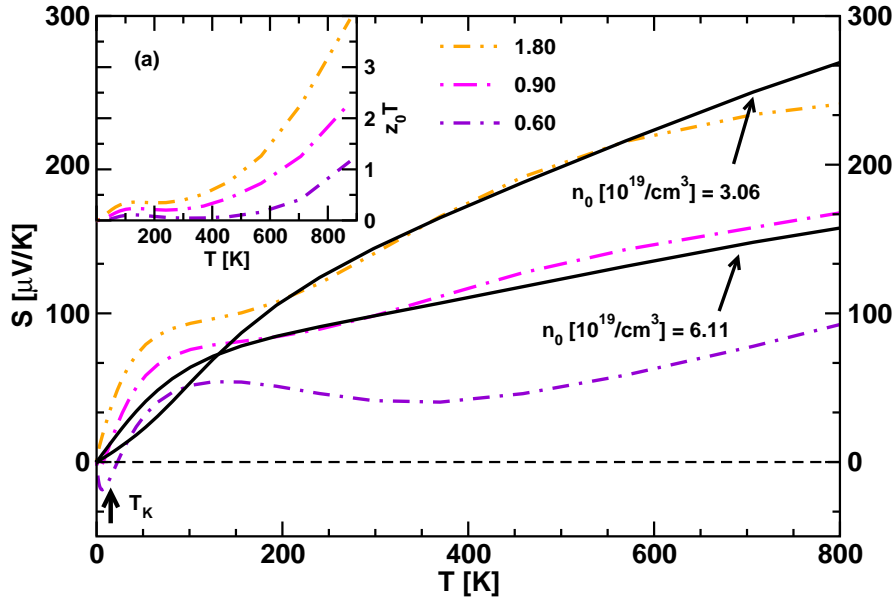


**Fig. 4** Main panel: Thermopower  $S$  versus temperature at different Tl concentrations  $x$  (in %, see legend) in the highly doped regime  $x > x_c$ . The two solid lines labeled by  $n_0$  correspond to  $S$  for the two highest doped cases (i.e. for  $x = 0.9$  and  $x = 1.8$ ) assuming a constant transport time. Inset (a) shows the temperature dependence of the dimensionless electronic figure of merit  $z_0T$  for  $x > x_c = 0.3$  (in %, see legends). This is indicative of trends only, since the lattice contribution to the thermal conductivity has been neglected in  $z_0T$ . The vertical arrow denotes the particular choice of Kondo temperature  $T_K = 14\text{K}$  made in this paper (see discussion in Sec. 4).

Within our model calculations, the charge Kondo contribution to the thermopower at low temperatures competes with the main contribution coming from the band instead of supplementing it. However, the contribution from the charge Kondo effect is generically quite large, and can reach values of order  $76\mu\text{V/K}$  for splittings  $\delta(\mu)/T_K > 1$ . This is indicated in Fig. 5 for the charge Kondo thermopower of the negative- $U$  Anderson impurity model [29] using a flat band appropriate for impuri-

ties in metallic systems. Hence, in principle, impurities exhibiting the charge Kondo effect could enhance the overall thermopower by the above value. This could offer a route to further improving the thermoelectric properties of appropriate materials.

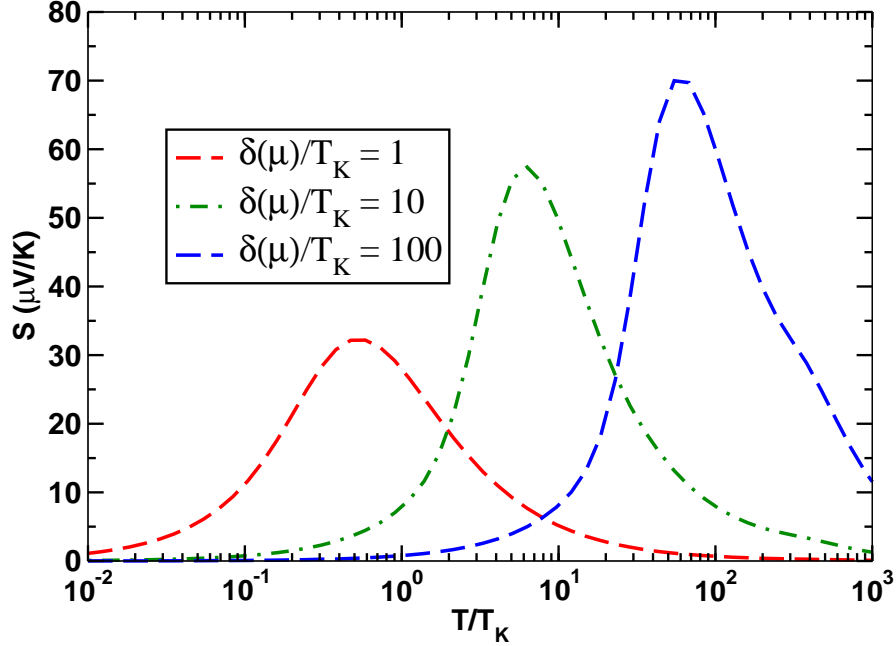


**Fig. 5** Thermopower  $S$  versus reduced temperature  $T/T_K$  of the negative- $U$  Anderson impurity model in a metallic host [29] for  $|U|/\Delta_0 = 8$  and several values of the charge splitting  $\delta(\mu)$ . The latter is defined as the splitting between the empty and doubly occupied states of the negative- $U$  Anderson impurity model and is analogous to the self-consistently calculated  $\delta(\mu)$  for the TI impurities in PbTe discussed in this paper.  $T_K$  denotes the Kondo scale. The charge Kondo effect provides a mechanism for large thermopowers of order  $k_B/e \approx 76 \mu\text{V/K}$  at charge splittings  $\delta(\mu)/T_K \geq 1$ . Since  $T_K$  can be made small, due to its exponential dependence on  $U$  and  $\Delta_0$ , such splittings are accessible in potential realizations of the charge Kondo effect, e.g. in negative- $U$  centers in semiconductors or in molecular junctions [29].

## 10 Conclusions

In summary, we investigated the low temperature properties of  $\text{Pb}_{1-x}\text{TI}_x\text{Te}$  within a model of TI impurities acting as negative  $U$  centers. Our NRG calculations explain a number of low temperature anomalies of  $\text{Pb}_{1-x}\text{TI}_x\text{Te}$ , including the qualitatively different behavior below and above the critical concentration  $x_c$ , where  $x_c \approx 0.3\%$ . They support the suggestion that the charge Kondo effect is realized in  $\text{Pb}_{1-x}\text{TI}_x\text{Te}$  [23, 32]. At  $x = x_c$ , two nonmagnetic valence states of TI become almost degen-

erate and the ensuing pseudospin charge Kondo effect results in a Kondo anomaly in the resistivity for  $x > x_c$  and a residual resistivity approximately linear in  $x$ . Our results for these quantities and the carrier density  $n_0(x)$  are in good qualitative agreement with experiments [23, 19, 22, 20]. For the Tl  $s$ -electron spectral function, we predict that one peak should be present far below  $E_F$  for  $x < x_c$  and that a second temperature dependent Kondo resonance peak develops close to, but below  $E_F$ , on increasing  $x$  above  $x_c$ . This provides a new interpretation of measured tunneling spectra[20], which could be tested by temperature dependent studies of tunneling or photoemission spectra. We also showed that the competing charge Kondo and band contributions to the low temperature thermopower imply that there are sign changes in the thermopower at low Tl concentrations. Investigating these in detail, particularly at  $x < 0.3\%$ , could shed further light on the charge Kondo effect in this system. In the future, it would be interesting to extend this work to investigate the effects of disorder, phonons, light and heavy hole bands, and non-resonant scattering channels on the thermoelectric properties of Tl doped PbTe.

**Acknowledgements** We thank K. M. Seemann, D. J. Singh, H. Murakami, P. Coleman, G. Kotliar, J. Schmalian, and I. R. Fisher for discussions and D. J. Singh, H. Murakami and I. R. Fisher for data [9, 19]. V.Z. acknowledges support by Croatian MZOS Grant No.0035-0352843-2849, NSF Grant DMR-1006605 and Forschungszentrum Jülich. T. A. C. acknowledges supercomputer support from the John von Neumann Institute for Computing (Jülich).

## References

1. H. B. Callen, 2nd. edn. *Thermodynamics and an Introduction to Thermostatistics* (John Wiley & Sons, New York, 1985).
2. A. F. Ioffe, *Semiconductor Thermoelements and Thermoelectric Cooling*, (Infosearch, London, 1954).
3. G. J. Snyder and E. S. Tober, *Nature Mat.* **7**, 105 (2008).
4. M. G. Kanatzidis, *Chem. Mater.* **22**, 648 (2010).
5. A.J. Minnich, M. S. Dresselhaus, Z. F. Ren, and G. Chen, *Energy Environ. Sci.* **2**, 466 (2009).
6. G. D. Mahan, *Solid State Phys.* **51**, 82 (1997).
7. L. D. Hicks and M. S. Dresselhaus, *Phys. Rev. B* **47**, 12727 (1993).
8. G. D. Mahan and J. O. Sofo, *Proc. Natl. Acad. Sci. USA* **93**, 7436 (1996).
9. D. J. Singh, *Phys. Rev. B* **81**, 195217 (2010).
10. V. Zlatić and R. Monnier, *Phys. Rev. B* **71**, 165109 (2005).
11. I. Terasaki, Y. Sasago, and K. Uchinokura, *Phys. Rev. B* **56**, R12685 (1997).
12. P. Wissgott, A. Toschi, H. Usui, K. Kuroki, and K. Held, *Phys. Rev. B* **82**, 201106 (2010).
13. A. Bentien et al., *Phys. Rev. B* **74**, 205105 (2006).
14. B. C. Sales et al., *Phys. Rev. B* **50**, 8207 (1994).
15. S. A. Némov and Yu. I. Ravich, *Phys. Usp.* **41**, 735 (1998).
16. B. A. Volkov, L. I. Ryabova, and D. R. Khokhlov, *Phys. Usp.* **45**, 819 (2002).
17. J. P. Heremans et al., *Science* **321**, 554 (2008).
18. I. A. Chernik and S. N. Lykov, *Sov. Phys. Solid State*, **23**, 817 (1981).
19. Y. Matsushita, P. A. Wiancki, A. T. Sommer, T. H. Geballe, and I. R. Fisher, *Phys. Rev. B* **74**, 134512 (2006).
20. H. Murakami, W. Hattori, Y. Mizomata, and R. Aoki, *Physica C* **273**, 41 (1996).
21. V. I. Kaidanov, S. A. Rykov, and M. A. Rykova, *Sov. Phys. Solid State* **31**, 1316 (1989).

22. M. Matusiak, E. M. Tunncliffe, J. R. Cooper, Y. Matsushita, and I. R. Fisher, Phys. Rev. B **80**, 220403 (2009).
23. Y. Matsushita, H. Bluhm, T. H. Geballe, and I. R. Fisher, Phys. Rev. Lett. **94**, 157002 (2005).
24. S. Ahmad, S. D. Mahanti, K. Hoang, and M. G. Kanatzidis, Phys. Rev. B **74**, 155205 (2006); K. Xiong, G. Lee, R. P. Gupta, W. Wang, B. E. Gnade, and K. Cho, J. Phys. D: Appl. Phys. **43**, 405403 (2010).
25. I. A. Drabkin and B. Ya. Moizhes, Sov. Phys. Semicond. **15**, 357 (1981).
26. K. Weiser, A. Klein, and M. Ainhorn, Appl. Phys. Lett. **34**, 607 (1979).
27. P. W. Anderson, Phys. Rev. Lett. **34**, 953 (1975).
28. A. Taraphder and P. Coleman, Phys. Rev. Lett. **66**, 2814 (1991).
29. S. Andergassen, T. A. Costi, and V. Zlatić, Phys. Rev. B **84**, 241107(R) (2011).
30. A. S. Erickson, N. P. Breznay, E. A. Nowadnick, T. H. Geballe, and I. R. Fisher, Phys. Rev. B **81**, 134521 (2010).
31. A. G. Mal'shukov, Solid State Commun. **77**, 57 (1991).
32. M. Dzero and J. Schmalian, Phys. Rev. Lett. **94**, 157003 (2005).
33. T. A. Costi, and V. Zlatić, Phys. Rev. Lett. **108**, 036402 (2012).
34. A. L. Shelankov, Solid State Commun. **62**, 327 (1987).
35. I. Martin and P. Phillips, Phys. Rev. B **56**, 14650 (1997).
36. K. Nakayama, T. Sato, T. Takahashi, and H. Murakami, Phys. Rev. Lett. **100**, 227004 (2008).
37. K. G. Wilson, Rev. Mod. Phys. **47**, 773 (1975); R. Bulla, T. A. Costi, and T. Pruschke, Rev. Mod. Phys. **80**, 395 (2008).
38. G. D. Mahan, 2nd. edn. *Many-Particle Physics*, (Plenum, New York, 1990).
39. T. A. Costi, A. C. Hewson, and V. Zlatić, J. Phys.: Condens. Matter **6**, 2519 (1994).
40. A. C. Hewson, 2nd. edn. *The Kondo Problem to Heavy Fermions*, Cambridge Studies in Magnetism (Cambridge University Press, Cambridge, U.K., 1997).
41. G. Iche and A. Zawadowski, Solid State Commun. **10**, 1001 (1972); A. C. Hewson, J. Bauer, and W. Koller, Phys. Rev. B **73**, 045117 (2006).
42. H. Sitter, K. Lischka, and H. Heinrich, Phys. Rev. B **16**, 680 (1977).